

## Fluid Flow Behavior of a Binary Mixture Under the Influence of External Disturbances Using Different Density Models

A. Parsa<sup>1</sup> and M.Z. Saghir<sup>1</sup>

**Abstract:** Experiments onboard the International Space Station typically display undesired convective flow as a results of unwanted oscillatory g-jitters. A cubic rigid cell filled with water (90%) and isopropanol (10%) with a thermal gradient and forced vibrations is considered. The cell is under the influence of three different levels of periodic oscillation ( $Ra_{vib} \approx 1.6, 650$  and  $4000$ ) applied perpendicular to the temperature gradient. In this paper, we examine the transport process (fluid flow, heat transfer and mass transfer) due to oscillatory g-jitters in the presence of Soret effect. The full transient Navier Stokes equations coupled with the mass and heat transfer formulation are solved numerically using a finite volume technique. The physical properties of the fluid mixture such as density are determined using two different models, (i) the PCSAFT equation of state and (ii) the mass weighted mixing rule. The results of each model for the flow, temperature and concentration distributions are compared and analyzed in detail. Results show a significant effect of the selected density model on the flow pattern and components separation especially when subjected to vibrations with higher Rayleigh number.

### Nomenclature

$c_0$	initial water concentration (carrier)	
$c$	transported component mass fraction	
$c_p$	mixture specific heat	$J \cdot kg^{-1} \cdot K^{-1}$
$D_C$	mass diffusion coefficient	$m^2 \cdot s^{-1}$
$D_T$	thermal diffusion coefficient	$m^2 \cdot s^{-1} \cdot K^{-1}$
$f$	frequency of the g-jitter	Hz
$\omega$	period of oscillation	s
$A$	amplitude of the oscillatory g-jitter	m
$\beta_T$	thermal volume expansion coefficient	$K^{-1}$

---

<sup>1</sup> Ryerson University, Department of Mechanical Engineering, 350 Victoria Street, Toronto, ON, L6H5C2, Canada

$J$	diffusion flux	$\text{kg}\cdot\text{m}^{-2}\cdot\text{s}^{-1}$
$k$	mixture thermal conductivity	$\text{W}\cdot\text{m}^{-1}\cdot\text{K}^{-1}$
$L$	cavity length	mm
$p$	pressure	Pa
$t$	time	s
$t_{vs}$	viscous time	s
$t_{th}$	thermal time	s
$T$	temperature	K
$T'$	period of oscillation	s
$T_{cold}$	cold wall temperature	K
$T_{hot}$	hot wall temperature	K
$T_m$	average temperature	K
$u$	velocity component in x-direction	$\text{m}\cdot\text{s}^{-1}$
$v$	velocity component in y-direction	$\text{m}\cdot\text{s}^{-1}$
$\mu$	mixture dynamic viscosity	$\text{kg}\cdot\text{m}^{-1}\cdot\text{s}^{-1}$
$\sigma$	mixture kinematic viscosity	$\text{m}^2\cdot\text{s}$
$\rho$	mixture mass density	$\text{kg}\cdot\text{m}^{-3}$
$\phi$	thermal diffusivity	$\text{m}^2\cdot\text{s}$

## 1 Introduction

Thermodiffusion or Soret effect is a molecular transport associated with a thermal gradient which creates concentration gradient in a mixture. Molecular diffusion takes place due to the concentration gradient in a mixture. A steady state is obtained when the separating effect of thermodiffusion is balanced by the remixing effect of molecular diffusion.

Precise measurements of the diffusion and Soret coefficients require repression of macroscopic flows in the mixtures. However, this is quite difficult in terrestrial conditions because of the thermal and solutal convection and double-diffusive instability. Space flight conditions are also producing vibrations (g-jitters) which can lead to significant macroscopic flows. The background g-jitter encountered in many space experiments may alter the benefits of the microgravity environment. Thus a study of the effects of controlled vibrations on the measurements of diffusion and Soret coefficients in liquid systems could be beneficial. This makes it important to perform theoretical and numerical studies of the vibration influence on temperature and concentration fields in diffusive mixtures.

It is known that the effects of vibration on a fluid system subjected to a density gradient that results from non uniform temperature field are relative flows inside the fluid which are called thermovibrational convection. The relative motions result

from different inertia of cold and hot parts of the fluid, which have different density. A 'pure' thermovibrational convective mechanism can be observed in weightlessness only as a result of eliminating static gravity which can provide an additional driving force for convective motion. These flow fields can be decomposed into the "quick" part, which oscillates with the frequency of vibration, and the "slow" time-average part (mean flow). The latter represents a non-linear response of the fluid to a periodic excitation.

Vibrational convection provides a mechanism of heat and mass transfer as a result of the mean flows. In weightlessness, this can be an additional way of transporting heat and matter (Beysens, 2006). In addition, there are many other important processes where thermal diffusion plays a critical role. The particular examples are thermohaline convection in oceans driven by salinity gradients associated with temperature differences (Schmitt, 1994), Isotope separation in liquid and gaseous mixtures (Furry, Jones, and Onsager, 1939) characterization and separation of polymers (Schimpf, 2000). In the analysis of the distribution of components in oil reservoirs, thermodiffusion effect together with isothermal and pressure diffusion are important (Ghorayeb and Firoozabadi, 2000).

Lyubimova *et al.* (Lyubimova, Shklyaeva, Legros, and Shevtsova, 2005) numerically investigated the effect of static and vibrational acceleration on the measurement of diffusion and Soret coefficients in binary mixtures, in low gravity conditions. The effect of vibrations applied in two directions, perpendicular and parallel to the imposed temperature gradient was investigated numerically. The study was performed for both zero gravity and low gravity conditions. It was found that a residual flow would exist which can be damped by applying an appropriate vibration intensity in the appropriate direction.

Melnikov *et al.* (Melnikov, Shevtsova, and Legros, 2008) studied the impact of two types of ideal sinusoidal vibrations at start up of thermovibrational convective flow. The development of thermovibrational convection in a cubic cell filled with isopropanol was investigated. It was shown that the initial vibrational phase plays a significant role in the transient behavior of thermovibrational convective flow. It was found that under the cosine vibrations, the flow reaches the steady state two times longer than sine vibrations and Nusselt number is almost ten times smaller. The flow and temperature fields were also investigated and compared in the two cases. It was shown that starting with sine accelerations causes significantly larger initial transport, than if the accelerations start as a cosine function.

Shevtsova *et al.* (Shevtsova, Gaponenko, Melnikov, Ryzhkov, and Mialdun, 2010) have studied the thermoconvective flows in an experimental test of convection caused by translational vibration of non-uniformly heated fluid in low gravity. The temperature fields were observed from the examined cubic cell and studied in wide

range of frequencies and amplitudes. It was confirmed that vibrational convection intensifies the heat transfer in the system. This transport was found to be significantly weaker in the absence of vibration and negligibly small in normal gravity for the studied levels of vibrations. In addition, by utilizing particle tracing in the experiment, the previous mean flow structures from the numerical studies were verified.

Yan *et al.* (Yan, Shevtsova, and Saghir, 2006) have performed a numerical study on the effect of low frequency g-jitter and static gravity on the thermodiffusion phenomenon. It was shown that the overall effect of vibrations on diffusion can be related to a nonlinear interaction between the effects caused by each individual g-jitter component. In the presence of large static gravity, the Soret separation is overshadowed by the convection in the mixture. In other words, the accuracy of the diffusion measurement will be affected significantly. The importance of periodic vibration on diffusion depends on the frequency. Low frequency vibrations such as g-jitters ranging from 0.001Hz to 0.025Hz have more effect on diffusion measurements when compared to the high frequency vibration. It was also found that static residual gravity simultaneously with the oscillatory g-jitter component in the direction perpendicular to the temperature gradient intensifies the flow field.

Later Yan *et al.* (Yan, Pan, Jules, and Saghir, 2007) studied the thermodiffusion process under different microgravity environments using measured g-jitter data from onboard the International Space Station (ISS) and FOTON-12. It was found that the diffusion process is only slightly affected by the g-jitters in both platforms. It was concluded that a proper choice of experimental location is of great importance in minimizing the effect of g-jitters. It was also shown that the undesirable effect of large oscillatory g-jitters similar to the quasi steady residual-g should be controlled. However, it is important to indicate that the data collected from the International Space Station (ISS) g-jitter measurement were obtained when the ISS was not in full assembly.

Recently Yan *et al.* (Yan, Jules, and Saghir, 2007) studied the effect of g-jitter on thermodiffusion on-board the International Space Station. It was found that the ISS microgravity environment can disturb the diffusion process from the ideal condition in some circumstances depending on the magnitude of the g-jitter. It was also shown that frequency and alignment of the experimental cell are both equally important.

The effect of average vibrational convection produced by high-frequency vibrations has been considered by Gershuni *et al.* (Gershuni, Kolesnikov, Legros, and Myznikova, 1997) in a binary mixture in the presence of Soret effect. The vibration frequency assumed to be high enough such that the period to be small with respect to all the reference hydrodynamic and thermal times. The analysis shows

interesting distinctive features. Two flow structures regimes were observed, in the main regime a four-vortex behaviour and in a secondary regime a one vortex behaviour. The dependence of the dimensionless heat flux (Nusselt number) on the vibrational Rayleigh number is presented for the two possible flow structures. It was also found that the structures are very sensitive to the variations of the Prandtl number.

Savino and Monti (Savino and Monti, 1999) studied the diffusion process in isothermal condition and a detailed analysis of vibrational impact on fluid physics experiments onboard microgravity platforms. It was shown that convective disturbances are related to both amplitude and frequency of vibrations and to the mutual orientation of density gradient and acceleration vector. It has been indicated that significant differences is found to the flow field arrangements and the time profiles of the thermofluid dynamic distortions in the two cases of natural convection "residual-g" and vibrational convection "g-jitters".

Thermodiffusion in a binary mixture of methane and n-butane subject to g-jitters was investigated by Chacha *et al.* (Chacha, Faruque, Saghir, and Legros, 2002). They found that the g-jitter produces mixing and affect the Soret effect in the cavity. The flow shows synchronously respond to the oscillatory accelerations. Later Chacha and Saghir (Chacha and Saghir, 2005) studied the effect of the time-dependent vertical gravity vector in a rectangular cell on the mass diffusion in a binary fluid mixture subject to a lateral temperature gradient. The effect of varying diffusion coefficients with the temperature and the fluid composition were analysed and compared to the average constant values. The numerical study shows the reduction of the compositional variation as a result of the increased convection produced by the g-jitter. They also found that the Soret coefficient oscillates with time at the same frequency as the original excitation. However, the backflow produce some disturbances which makes it non-sinusoidal in shape.

Shevtsova *et al.* (Shevtsova, Melnikov, Legros, Yan, Saghir, Lyubimova, Sedelnikov, and Roux, 2007) examined the problem of diffusion and vibrational convection with the Soret effect in a cubic cell subjected to a temperature difference between opposite lateral walls and filled with the related binary mixture of water (90%) and isopropanol (10%). Numerical simulations were performed for g-jitter induced flow when the direction of g-jitter was the same as the residual gravity vector and perpendicular to the applied temperature gradient. All the physical properties including the diffusion coefficients ( $D_C$  and  $D_T$ ) were assumed constant. Different combinations of static and oscillatory vibrations with two different frequencies were examined. Component separation as a result of the Soret effect according to the driving actions was analyzed. By using the concept of time averaged model, the interactions between the mean and fluctuating motions was discussed.

In this paper, we study the effect of vibration (g-jitter) and Soret effect in a fluid mixture by performing a direct numerical analysis of the transient processes using the finite volume method. The effects of variable parameters such as density under the influence of three different levels of vibrational condition were studied. We consider a finite two-dimensional cavity filled with a binary mixture of water and isopropanol ( $C_3H_7OH$ ) and is subjected to a temperature gradient normal to the vibrational force (g-jitter). The mathematical formulation of the problem in dimensional form is introduced in Section 2. In our mathematical model the fluid density can be varying with the temperature and fluid composition. Section 3 describes the geometrical model, boundary and initial conditions. Section 4 presents the numerical procedure adopted for the problem solution as well as the code validation process. In Section 5, we discuss the results obtained from different cases by using the referred equation of state models. Section 6 concludes the results of the study.

## 2 Governing Equations

A complete set of governing equations have been used to simulate the thermo-solutal diffusion and convection. It consists of the mass conservation equation, momentum equation and the energy equation. In addition, PC-SAFT EOS (Pan, Jiang, Yan, Kawaji, and Saghir, 2007), and mass weighted mixing rule were used for calculating the density. The solved equations are as follows;

### 2.1 Mass conservation equation

The following equation is used for the mass conservation in the fluid which comprised of two components, isopropanol with mass fraction of  $c$  and water, the carrier fluid, with mass fraction being equal to  $c_0 = 1 - c$ .

$$\frac{\partial \rho}{\partial t} + \frac{\partial \rho u}{\partial x} + \frac{\partial \rho v}{\partial y} = 0 \quad (1)$$

Where  $\rho$  is the density,  $u$  and  $v$  are the velocity component in the  $x$  and  $y$  directions respectively, and  $t$  marks the time.

For the solute and in terms of its mass fraction  $c$ , the principle of mass conservation results in:

$$\begin{aligned} \frac{\partial}{\partial t}(\rho c) + \frac{\partial}{\partial x}(\rho u c) + \frac{\partial}{\partial y}(\rho v c) \\ = \frac{\partial}{\partial x} \left[ \rho (D_c \frac{\partial c}{\partial x} + D_T \frac{\partial T}{\partial x}) \right] + \frac{\partial}{\partial y} \left[ \rho (D_c \frac{\partial c}{\partial y} + D_T \frac{\partial T}{\partial y}) \right] \end{aligned} \quad (2)$$

The terms  $D_C$  and  $D_T$  are the mass diffusion coefficient and the thermodiffusion coefficient respectively. They were assumed constant as shown in Table 1. Density is varying by being calculated either from PC-SAFT Equation of State or by the mass weighted mixing rule.

## 2.2 Momentum conservation equation

The Navier–Stokes equations are used to solve the velocity field. The equation in the x direction is written as:

$$\frac{\partial}{\partial t}(\rho u) + \frac{\partial}{\partial x}(\rho uu) + \frac{\partial}{\partial y}(\rho vu) = -\frac{\partial p}{\partial x} + \frac{\partial}{\partial x} \left[ \mu \left( \frac{\partial u}{\partial x} \right) \right] + \frac{\partial}{\partial y} \left[ \mu \left( \frac{\partial u}{\partial y} \right) \right] + \rho g_x \quad (3)$$

and in the y direction:

$$\frac{\partial}{\partial t}(\rho v) + \frac{\partial}{\partial x}(\rho uv) + \frac{\partial}{\partial y}(\rho vv) = -\frac{\partial p}{\partial y} + \frac{\partial}{\partial x} \left[ \mu \left( \frac{\partial v}{\partial x} \right) \right] + \frac{\partial}{\partial y} \left[ \mu \left( \frac{\partial v}{\partial y} \right) \right] \quad (4)$$

Where

$$g_x = -A\omega^2 \cos(\omega t), \quad \omega = 2\pi f$$

The vibration is applied only in the  $x$  direction. The static gravity is set equal to zero, while  $A$  is the amplitude of the applied oscillating part (g-jitter) and  $f$  is the frequency of oscillation ( $\omega$  is the angular frequency). The pressure is marked by  $p$  and  $\mu$  is the dynamic viscosity of the mixture.

The mixture dynamic viscosity  $\mu$  at each node is computed based on mass fraction average of the pure species viscosities:

$$\mu = \int_i c_i \mu_i \quad (5)$$

Where  $c_i$  is the mass fraction of each component at each node and  $\mu_i$  is the pure components viscosities.

## 2.3 Energy conservation equation

Assuming no internal heat source, the conservation of thermal energy is written as follows:

$$\frac{\partial}{\partial t}(\rho T) + \frac{\partial}{\partial x}(\rho u T) + \frac{\partial}{\partial y}(\rho v T) = \frac{\partial}{\partial x} \left[ \frac{k}{c_p} \left( \frac{\partial T}{\partial x} \right) \right] + \frac{\partial}{\partial y} \left[ \frac{k}{c_p} \left( \frac{\partial T}{\partial y} \right) \right] \quad (6)$$

Where  $c_p$  is the specific heat,  $k$  is the thermal conductivity and  $t$  is the temperature of the fluid.

## 2.4 Density models

PC-SAFT equation of state is used to determine the density of the mixture as well as the fugacity which is needed to estimate the diffusion coefficients. The calculation were performed at each node of the grid and re-calculated for each time step. Further detail on the usage of this equation is found in Pan, Jiang, Yan, Kawaji, and Saghir (2007). For the second model, the density is calculated using the mass weighted mixing rule and considered as a function of concentration.

$$\rho = \frac{1}{\int_i \frac{c_i}{\rho_i}} \quad (7)$$

Where  $c_i$  is the mass fraction of the components at each node and  $\rho_i$  is the pure components density. As shown in this equation, there is no direct relation between temperature and density in this model. However, there is an indirect connection through the mass conservation equation and thermodiffusion (i.e. equation 2) results from components concentration variations in the domain. Unlikely, in the PC-SAFT model, there is a direct coupling between temperature and concentration through the equation of state.

## 3 Gometrical model, physical properties, boundary and initial conditions

The physical model of the cavity under study is sketched in Figure 1. The system consists of a square cavity with the length being equal to 0.01 m, containing the binary mixture of water, the heavier component, with initial mass fraction of  $c_0$  (i.e. 0.9) and the isopropanol with a mass fraction of  $c$  (i.e. 0.1).

The physical properties for each component and other coefficients used in the analysis were extracted from Reference (Pan, Jiang, Yan, Kawaji, and Saghir, 2007) in order to have comparable results in terms of diffusion coefficients. The cavity is subject to the oscillatory component of the gravity called g-jitter which modeled by a harmonic contribution to the body force. It is considered perpendicular to the thermal gradient and coincides with the  $x$  axis. The opposite walls are kept at constant temperatures,  $T_{hot}$  and  $T_{cold}$ , so the temperature difference would be  $\Delta T = T_{hot} - T_{cold}$ . All other walls are assumed thermally insulated, rigid and impermeable. The applied boundary conditions are shown in Figure 1 and are as follows:

At  $x = 0, x = L$  :

$$u = 0 \quad (8)$$

$$J_x = D_C \frac{\partial c}{\partial x} + D_T \frac{\partial T}{\partial x} = 0 \quad (9)$$

$$T = \begin{cases} x = 0, & T_{hot} \\ x = L, & T_{cold} \end{cases} \quad (10)$$

At  $y = 0, y = H$  :

$$v = 0 \quad (11)$$

$$J_y = D_C \frac{\partial c}{\partial y} + D_T \frac{\partial T}{\partial y} = 0 \quad (12)$$

$$\frac{\partial T}{\partial y} = 0 \quad (13)$$

The velocities at all grid points are initially set equal to zero. The initial concentration of water ( $c_0=0.9$ ) is applied and the pressure ( $p_0 = 101325 Pa$ ) at the average temperature  $T_m = (T_{cold} + T_{hot})/2$  is calculated and used as an initial value.

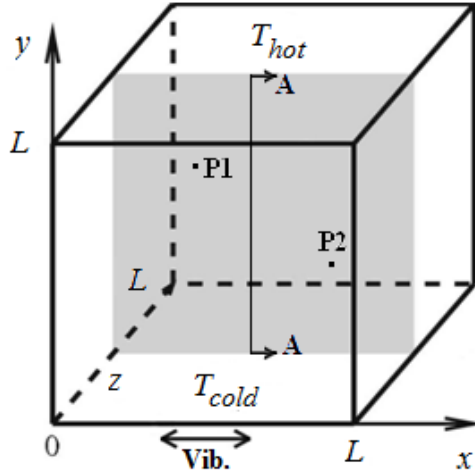


Figure 1: Geometry and coordinate system; the gray vertical cross section is used for the analysis

The analyses were performed at two points, P1 and P2 with the following coordinates:

$$P1 \left| \begin{array}{l} x = (\frac{1}{3})L \\ y = (\frac{2}{3})L \end{array} \right. \quad P2 \left| \begin{array}{l} x = (\frac{2}{3})L \\ y = (\frac{1}{3})L \end{array} \right. \quad (14)$$

In each case, the time step size ( $\Delta t$ ) is obtained from the referred period of oscillation and frequency by  $\Delta t = T'/10$  where  $T' = 1/f$ .

The physical properties of the mixture in the two studied models are given in Table 1 (Yan, Shevtsova, and Saghir, 2006; Shevtsova, Melnikov, Legros, Yan, Saghir, Lyubimova, Sedelnikov, and Roux, 2007):

Table 1: Physical properties of 90% water and 10% Isopropanol mixture

Physical properties	Mixing rule	PC-SAFT EOS
Diffusion coefficient [m <sup>2</sup> /s]	$7.77 \times 10^{-10}$	$7.77 \times 10^{-10}$
Thermal diffusion coefficient [m <sup>2</sup> /s.K]	$2.39 \times 10^{-13}$	$2.39 \times 10^{-13}$
Thermal diffusivity [m <sup>2</sup> /s]	$1.347 \times 10^{-7}$	$1.317 \times 10^{-7}$
Dynamic viscosity [kg/m.s]	$1.036 \times 10^{-3}$	$1.036 \times 10^{-3}$
Kinematic viscosity [m <sup>2</sup> /s]	$1.067 \times 10^{-6}$	$1.043 \times 10^{-6}$
Thermal conductivity [W/(m.K)]	0.522	0.522
Specific heat capacity [J/(kg.K)]	3990.5	3990.5
Mixture density [kg/m <sup>3</sup> ]	$970.8 \pm 0.1$	$993.3 \pm 6$

## 4 Numerical approach, convergence criteria and code validation

### 4.1 Numerical approach

In this analysis mass, momentum and energy equations are discretized by the finite volume method and the SIMPLE algorithm (Patankar, 1980) used for solving the continuity equation which is then used to update the pressure. In addition, primitive variables ( $u, v, p, T$ ) were employed. Afterwards, they are used to correct the velocity and pressure:

$$p = p^* + p', \quad \vec{v} = \vec{v}^* + \vec{v}' \quad (15)$$

In the above correlation equation,  $p^*$  is the initial guessed pressure which is corrected by  $p'$ . Correspondingly,  $v^*$  is the related velocity obtained from momentum equation. It is then corrected by  $v'$  achieved from following equations:

$$\vec{v}' = -K \cdot \nabla p', \quad K = \begin{pmatrix} K_x & 0 \\ 0 & K_y \end{pmatrix} \quad (16)$$

where  $K$  is a diagonal tensor resulting from the discretization scheme. The process continued until it meet the required convergence criteria. As a result of the strong coupled problem, when PC-SAFT EOS is used, density is calculated in terms of local temperature, pressure and concentration at each iterative step. The following

equation is used for the pressure correction and obtained from the continuity and equation 14:

$$\nabla \cdot (K \cdot \nabla p') = \nabla \cdot \vec{v}^* \quad (17)$$

Finally, the revised velocity is calculated from the following equation by using the correct  $p'$ .

$$\vec{v} = \vec{v}^* - K \cdot \nabla p' \quad (18)$$

#### 4.2 Convergence criteria and code validation

The convergence criteria is set  $10^{-6}$  and the relative error for all the unknowns ( $u, v, p, c, T$ ) is calculated from the following equation:

$$\Psi_F = \frac{1}{(n \cdot m)} \int_{i=1}^{i=m} \int_{j=1}^{j=n} \left| (T_{i,j}^{k,s+1} - T_{i,j}^{k,s}) / T_{i,j}^{k,s+1} \right| \quad (19)$$

The iteration number showed by  $s$  and  $k$  marks the time step. The grid coordinates are denoted by  $i$  and  $j$ . The density is calculated at each point of the grid and continually updated during the calculations procedure. The complete description of the algorithm can be found in Reference (Patankar, 1980) and (Peyret and Taylor, 1990).

The numerical code used in this work was benchmarked with other research groups (Shevtsova, Melnikov, Legros, Yan, Saghir, Lyubimova, Sedelnikov, and Roux, 2007). Results of all the groups showed good agreements. In addition, the code was validated with the analytical solution in the case where no vibration applied i.e. pure diffusion. The components separation between hot and cold walls up to reaching the steady state condition was analyzed. The following equation is used for the analytical solution (Mialdun and Shevtsova, 2008):

$$\Delta c(t) = \Delta c_{st} \left[ 1 - \frac{8}{\pi^2} \int_{n, odd}^{\infty} \frac{1}{n^2} \exp\left(-n^2 \frac{t}{t_D}\right) \right] \quad (20)$$

Where,  $\Delta c_{st}$  is the steady state separation or the maximum possible separation. Time is denoted by  $t$  and  $t_D$  is the diffusion time. The maximum separation occurs as a result of the presence of Soret effect and is calculated using the following equation:

$$\Delta c = -S_T c_0 (1 - c_0) \Delta T \quad (21)$$

Also, the mesh sensitivity analysis was performed to give confidence of the obtained results. Three meshes,  $10 \times 10$ (coarse),  $15 \times 15$ (normal) and  $31 \times 31$ (fine)

were generated. The cavity was subjected to a vibration with 1 Hz frequency and 0.07m amplitude, perpendicular to the imposed temperature gradient. The results were analyzed at two different characteristic times, viscous and thermal times. Velocity magnitude and components mass fraction along the middle vertical line (line AA in Figure 1) were used for the comparison. It was concluded that the  $15 \times 15$  mesh size is accurate enough for the analysis.

## 5 Results and discussion

Double diffusive convection in a binary mixture of isopropanol (10%) and water (90%) at zero gravity condition in the presence of Soret effect will create a concentration gradient due to the temperature gradients between the walls. The direction of the displacement for each component depends on the Soret coefficient sign. Based on the Pan *et al.* (Pan, Jiang, Yan, Kawaji, and Saghir, 2007) studies, for the current mixture, Soret coefficient is negative which results in high concentration of water in the hot side of the cavity.

Applying the external vibration on the cavity in a zero gravity condition makes the thermovibrational convection to produce an increase in the heat transfer and a decrease of the concentration gradient.

The vibrational analogue of Rayleigh number identified as  $Ra_{vib}$  (Rayleigh vibration) was used for defining the strength of the applied vibration:

$$Ra_{vib} = \frac{(A\omega\beta_T\Delta TL)^2}{2\sigma\phi} \quad (22)$$

Where  $A$  is the amplitude of vibrations,  $\omega = 2\pi f$  is the angular frequency,  $L$  is the characteristic size,  $\Delta t$  is the applied temperature difference,  $\beta_T$  is the thermal expansion coefficient,  $\nu$  is the kinematic viscosity and  $\phi$  is the thermal diffusivity.

The analysis was performed for three cases and in each case the mixing rule method and PC-SAFT EOS are used for calculating the density. In addition, two different characteristic times were used for the comparisons; at one viscous time ( $t_{vs} = L^2/\nu$ ) known as the time where the flow got affected by the vibration and at one thermal time ( $t_{th} = L^2/\phi$ ) that indicate the time where thermal equilibrium is established. Based on the density calculated from each model, it was found that the viscous and thermal times relative to each model are slightly different. In the coming graphs, the first value for the characteristic times is always calculated from mixing rule method and second time is related to the PC-SAFT EOS.

In the first case as shown in Table 2, the temperatures are set 293 K and 303 K for the cold and hot walls. The applied frequency and amplitudes are 0.05Hz and

0.07m respectively. As a result and based on the density calculated from the related model, the Rayleigh vibrations are 1.62 and 1.7 for mixing rule method and PC-SAFT EOS respectively. In the second case, the temperatures and amplitude remain unchanged but the frequency increased to 1Hz in order to achieve Rayleigh vibration equal to 646 and 679 respectively. The third case has the hot wall temperature set equal to 308 K, the frequency increased again to 2Hz and the amplitude is set to 0.057m. As a result, the Rayleigh vibrations are found to be 3857 and 4038 for the two studied models respectively.

Table 2: Three studied cases with different applied conditions

Properties	Case 1	Case 2	Case 3
Cold wall temperature [K]	293	293	293
Hot wall temperature [K]	303	303	308
G-jitter Frequency [Hz]	0.05	1	2
G-jitter Amplitude [mm]	70	70	57
Rayleigh Vibration	1.62/1.7 <sup>1</sup>	646/679 <sup>1</sup>	3857/4038 <sup>1</sup>

<sup>1</sup> Based on the density calculated from mixing rule method and PC-SAFT EOS

### 5.1 Case 1: Low Rayleigh vibration ( $Ra_{vib} = 1.62 / 1.7$ )

The temperature difference is set 10°K and a very low frequency of 0.05Hz is applied. The applied amplitude is also 0.07m. As a result, the Rayleigh vibrations are 1.62 and 1.7 for the two models.

The temperature and isopropanol mass fraction in the middle vertical line (Line AA in Figure 1) are plotted at one thermal time as shown in Figure 2.

The results show complete agreement between the two density models. When thermodiffusion is forcing the two components to separate between the hot and cold walls, the applied external vibration makes the components to mix. The flow created by the imposed vibration is weak so that it had no effect on the temperature distribution in the cavity. As such, linear temperature distribution is obtained regardless of the way the density is evaluated.

The instantaneous velocities at each node were averaged during the five periods after each characteristic time for better comparison. The mean velocity vector profiles for PC-SAFT EOS at one viscous and one thermal time are shown in Figure 3.

Based on the Gershuni theory (Gershuni and Lyubimov, 1998) the four cell pattern

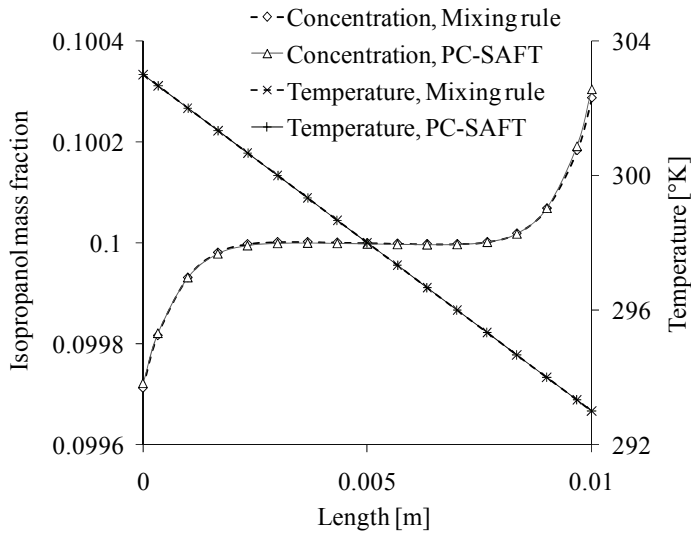
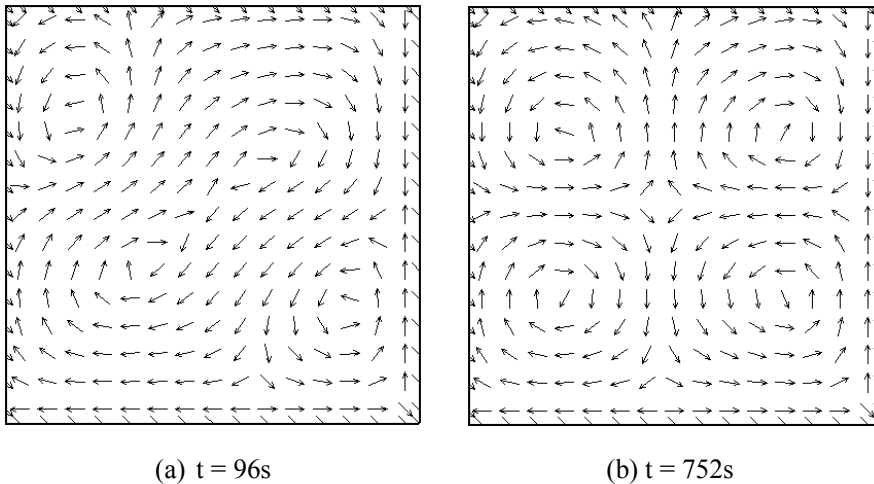


Figure 2: Temperature and isopropanol mass fraction at one thermal time ( $t=742s$  and  $752s$ )



(a)  $t = 96s$

(b)  $t = 752s$

Figure 3: Mean velocity vector profile at one viscous time,  $t=96s$  and at one thermal time,  $t=752s$  using PC-SAFT EOS

was detected regardless of the time selected. Figure 3 shows the four cell flow pattern using PC-SAFT EOS which is in agreement with Gershuni theory. However, such flow pattern was not obtained using mixing rule method.

In order to study the instantaneous variation of the parameters in the domain, two critical points, P1 and P2, were adopted as shown in Figure 1. The rate of change in density is plotted at point P1 for the two models as shown in Figure 4. They are about  $10^3$  times higher using PC-SAFT EOS when compared with mixing rule method. As expected, the rate of change of density is higher at the start up but reduced significantly after one viscous time. The approach for the density calculation with mixing rule shows no change in the density after one viscous time whereas for the density calculated using PC-SAFT EOS much higher rate of change during the whole process is found.

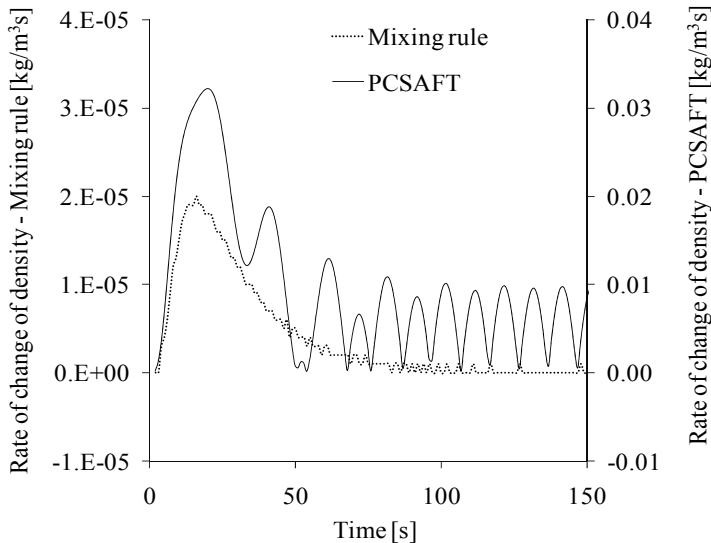


Figure 4: Rate of change of density at point P1 using mixing rule method and PC-SAFT EOS

This behavior makes the average velocity in the domain for PC-SAFT EOS to be much higher in comparison with mixing rule method. There is a  $10^4$  order of magnitude difference between the velocities in the two models with higher velocity when PC-SAFT EOS is used for the density. This behavior can be due to the link between instantaneous variations of density and temperature in the PC-SAFT

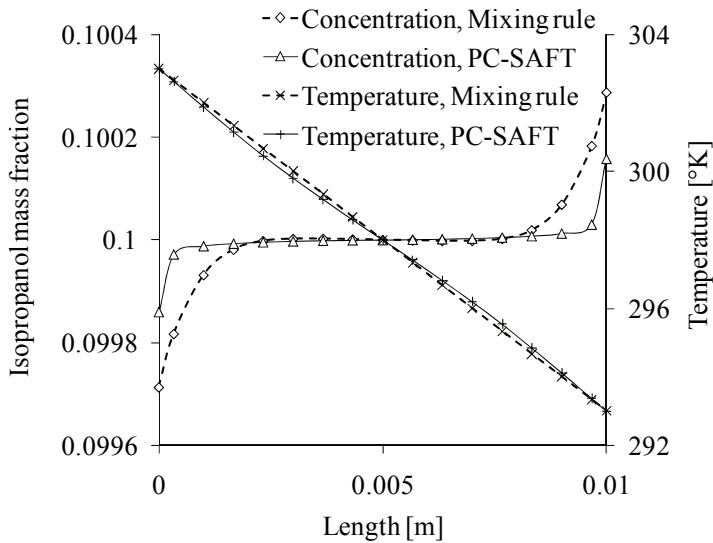


Figure 5: Temperature and isopropanol mass fraction at one thermal time ( $t=742s$  or  $752s$ )

EOS in comparison with mixing rule which has no direct link as stated in equation 7. Temperature instantaneous variation makes the density to fluctuate much more using PC-SAFT EOS in comparison with the mixing rule approach.

### 5.2 Case 2: Intermediate Rayleigh vibration ( $Ra_{vib} = 646 / 679$ )

In order to get higher Rayleigh vibration, the frequency is increased to 1 Hz. The temperature and amplitude are set the same as in the previous case. As a result, the Rayleigh vibration increased to about 646 and 679 based on the adopted density model. The temperature and isopropanol mass fraction line plots at one thermal time are shown in Figure 5.

Temperature profile is linear in mixing rule method at both characteristic times where PC-SAFT EOS shows some nonlinearity. This means temperature influenced by the external vibration when density calculated by PC-SAFT EOS. Concentration plots for isopropanol mass fraction also shows disagreement between the two models. Mixing rule method presents more components separation in comparison with PC-SAFT EOS. This difference is higher in one thermal time in comparison with one viscous time which indicates the increase in the disparity between the two models by the time.

The mean velocity vector profile during the 5 period for mixing rule method at one

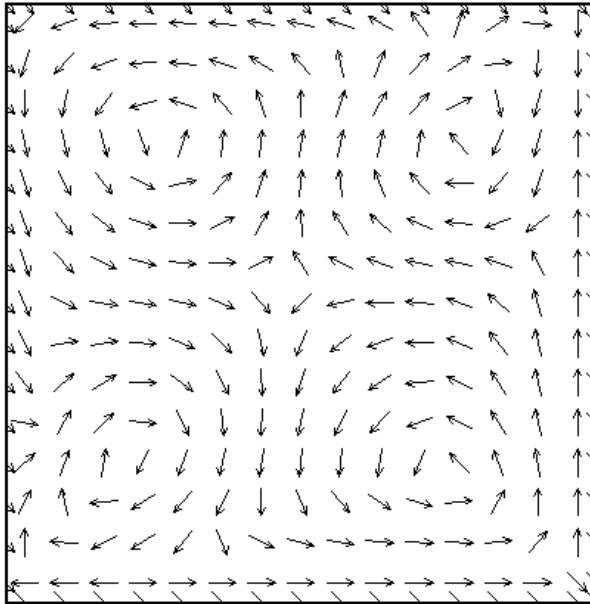


Figure 6: Mean velocity vector profile at one thermal time in mixing rule method (unsymmetrical four cell pattern)

viscous time could not predict the four cell pattern and at one thermal time shows unsymmetrical shape of the four cells as shown in Figure 6. Correspondingly, PC-SAFT EOS predicts the full symmetrical configuration of the four cell pattern at both one viscous and one thermal times as shown in Figure 3b.

The rate of change in density at point P1 for the two models is shown in Figure 7. They are about  $10^3$  times higher in PC-SAFT EOS compare with mixing rule method. Similar to the previous case, the rate of change of density is higher at start up but reduced significantly after one viscous time. The mixing rule method shows much less fluctuation in the density whereas PC-SAFT EOS has much higher rate of change of density.

The disagreements between the velocity vector profiles beside the average velocity magnitude differences between the two models can justify the disparities in the temperature and concentration plots in Figure 5. Similar to the previous case, there are about  $10^4$  order of magnitude differences between the average velocities in the two models. This behavior can be justified by the density and temperature link in the PC-SAFT EOS in comparison with mixing rule method. The later, as shown in equation 7, has no direct connection between the temperature and density. The

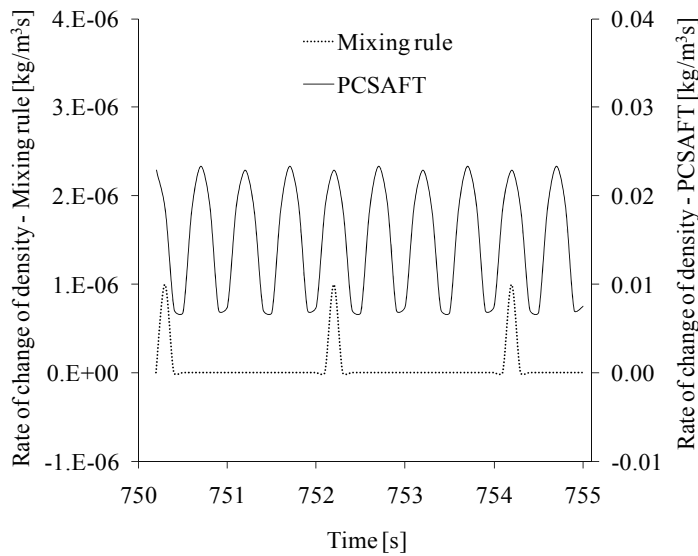


Figure 7: Rate of change of density at point P1 in mixing rule method and PC-SAFT EOS

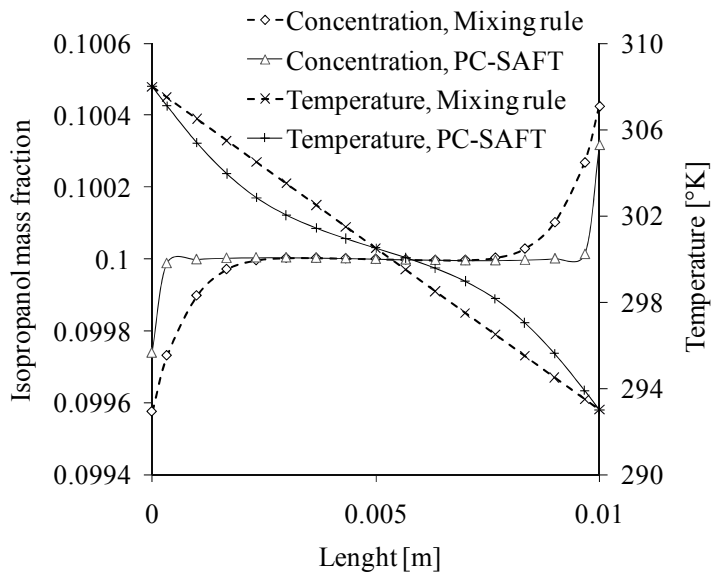


Figure 8: Temperature and isopropanol mass fraction at one thermal time ( $t=742s$  or  $752s$ )

density varied much more in PC-SAFT EOS in comparison with the mixing rule method.

The higher velocity magnitude in PC-SAFT EOS makes more powerful mixing that result in less component separation in comparison with mixing rule method as shown in Figure 5.

### 5.3 Case 3: High Rayleigh vibration ( $Ra_{vib}= 3857 / 4038$ )

In this case, Rayleigh vibration was set to be around 4000. The temperature and concentration plots in Figure 8 show complete disagreements between the two models. The temperature distribution in PC-SAFT EOS is completely distorted when it is still linear in mixing rule method.

The components separation at one thermal time is more pronounced using mixing rule method as shown in Figure 8. This is due to the strong mixing obtained by using the PC-SAFT EOS.

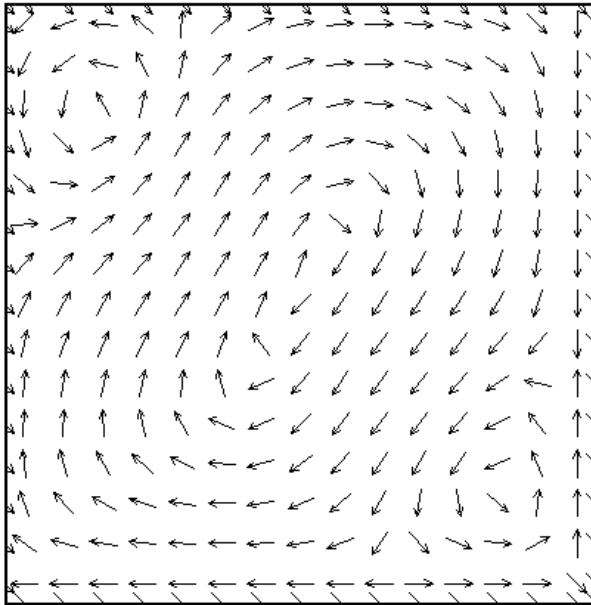


Figure 9: Mean velocity vector profile (One diagonal vortex pattern) at one thermal time in the PC-SAFT EOS

The four cell pattern is expected in this case as the Rayleigh vibration is below the critical value  $Ra_{cr}=8000$  (Gershuni and Lyubimov, 1998). Based on the Gershuni *et al.* (Gershuni and Lyubimov, 1998) above the critical value, the four cell pattern

should change to one diagonal and the temperature profile should be distorted. In PC-SAFT EOS, although the Rayleigh vibration is far below the critical value, unexpectedly the temperature profile significantly distorted and the one diagonal vortex pattern is obtained at one thermal time as shown in Figure 9. In the mixing rule method, as expected, the four cell pattern is observed at one thermal time.

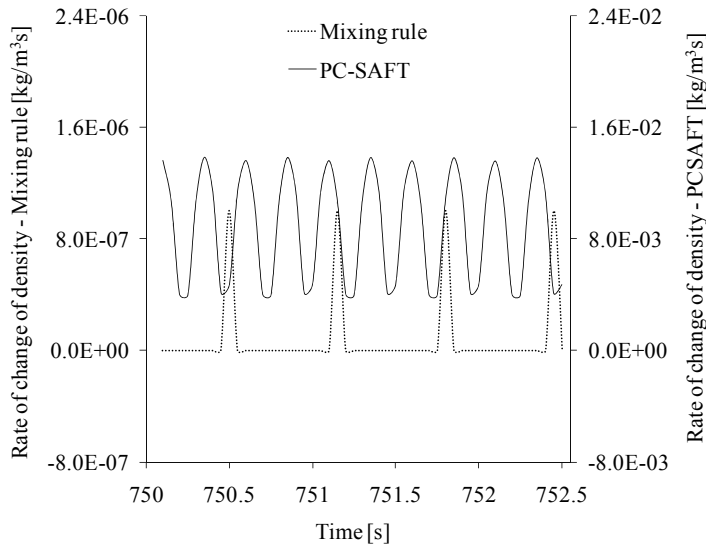


Figure 10: Rate of change of density at point P1 in mixing rule method and PC-SAFT EOS

The rate of change in density is plotted at point P1 for the two models as shown in Figure 10. They are about  $10^4$  times higher in PC-SAFT EOS compare to mixing rule method. The higher velocity magnitude in PC-SAFT EOS makes a powerful mixing and therefore less component separation noticed in comparison with the mixing rule method. Due to the mentioned differences between the rate of change of density, mean velocity vector profiles and the average velocity magnitudes, the temperature and concentration plots are quite different in this case for the two studied models as shown in Figure 8. This behavior can also be explained by the link between instantaneous variations of density and temperature in the PC-SAFT EOS model.

In PC-SAFT EOS, as shown in Figure 11, density and temperature are completely coupled. Unlike the two previous cases, there is a second change in the trend of temperature and density before getting completely steady. This happens before one

thermal time and more specifically between 400 and 800 seconds. This behavior can be due to the high Rayleigh vibration and as a result high velocity magnitude in this case. Accordingly, since they are strong enough, they can influence the composition and temperature isolines. Correspondingly, the transmission between four cell pattern and one diagonal which happens also between 400 and 800 seconds can be justified.

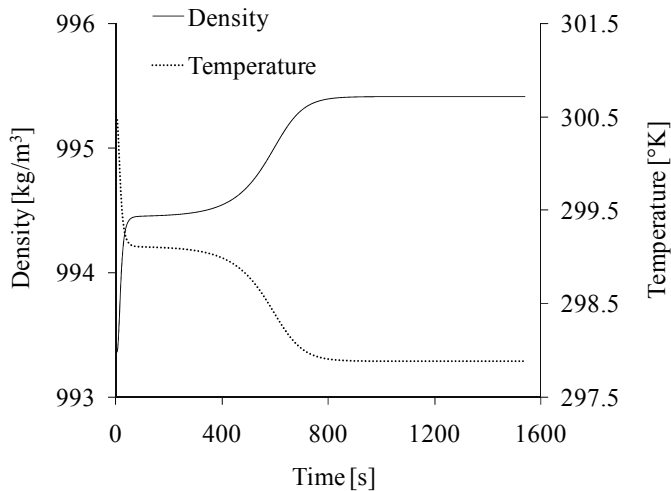


Figure 11: Density and temperature variation at point P1 in PC-SAFT EOS

## 6 Conclusion

Double-diffusive thermal convection with the Soret effect is considered in a cubic cell subjected to external vibrations. The structure of time-averaged (mean) fields was examined on a long time scale, i.e., during thermal time along with the composition and temperature profiles. Three different levels of Rayleigh vibrations were considered by using different frequencies, amplitudes and temperature gradients. Two models, weighted average mixing rule and PC-SAFT EOS were used for calculating density. It was found that using PC-SAFT EOS make the results more realistic in comparison with mixing rule method. It makes the formation of strong one diagonal flow pattern in Rayleigh vibrations less than the critical number Gershuni theory predicted. Accordingly, significant mixing occurs when using PC-SAFT EOS that results in deduction of components migration. The velocity magnitude is higher when density calculated using PC-SAFT EOS. It was found that the coupling between the temperature and density by using PC-SAFT EOS

make higher instantaneous change in the density. This will result in higher velocity magnitudes which then reflect in components separations.

## References

- Beysens, D.** (2006): Europhysics News 37, 22.
- Chacha, M.; Faruque, D.; Saghir, M. Z.; Legros, J. C.** (2002): Solutal thermodiffusion in binary mixture in the presence of g-jitter, *Int. J. Therm. Sci.*, vol. 41, p. 899.
- Chacha M.; Saghir, M. Z.** (2005): Solutal-thermo-diffusion convection in a vibrating rectangular cavity, *Int. J. Therm. Sci.*, vol. 44, p. 1.
- Furry, W.H.; Jones, R. C.; Onsager, L.** (1993): On the theory of isotope separation by thermal diffusion, *Phys. Rev.*, vol. 55, p.1083.
- Gershuni, G.Z.; Kolesnikov, A.K.; Legros, J.C.; Myznikova, B.I.** (1997): On the vibrational convective instability of a horizontal, binary-mixture layer with Soret effect, *J. Fluid Mech.*, vol. 330, p. 251.
- Gershuni, G.Z.; Lyubimov, D.V.** (1998): *Thermal vibrational convection*. Wiley, New York.
- Ghorayeb, K.; Firoozabadi, A.** (2000): Modeling multicomponent diffusion and convection in porous media, *SPEJ*, vol. 5, p. 158.
- Lyubimova, T.; Shklyaeva, E.; Legros, J.C.; Shevtsova, V.; Roux, B.** (2005): Numerical study of high frequency vibration influence on measurement of Soret and diffusion coefficients in low gravity conditions, *Advances in Space Research*, vol. 36, pp. 70–74
- Melnikov, D.; Shevtsova, V.; Legros, J.C.** (2008): Impact of conditions at start-up on thermovibrational convective flow, *Physical Review E*, vol. 78, p. 056306.
- Mialdun, A.; Shevtsova, V.** (2008): Development of optical digital interferometry technique for measurement of thermodiffusion coefficients. *Int. J. Heat Mass Transfer*, vol. 51, p. 3164.
- Pan, S.; Jiang, C.; Yan, Y.; Kawaji, M.; Saghir, M. Z.** (2007): Theoretical approach to evaluate thermodiffusion in aqueous alkanol solutions, *J. Chem. Phys.*, vol. 126, p. 014502.
- Patankar, S.V.** (1980): *Numerical Heat Transfer and Fluid Flow*, McGraw-Hill, New York.
- Peyret R.; Taylor, T.D.** (1990): *Computational Methods for Fluid Flow*, Springer - Verlag, Berlin.
- Savino, R.; Monti, R.** (1999): Convection induced by residual-g and g-jitters in

diffusion experiments, *Int. J. Heat Mass Transfer*, vol. 42, p. 111.

**Schimpf, M.E.** (2000): Thermal field-flow fractionation, *Field-Flow Fractionation Handbook*, Wiley, New York, p.239.

**Schmitt, R.** (1994): Double diffusion in oceanography, *Annual Rev. Fluid Mech.*, vol. 26, p. 255.

**Shevtsova, V.; Gaponenko, Y.; Melnikov, D.; Ryzhkov, I.; Mialdun, A.** (2010): Study of thermoconvective flows induced by vibrations in reduced gravity, *Acta Astronautica*, vol. 66, pp. 166–173.

**Shevtsova, V.; Melnikov, D.; Legros, J.C.; Yan, Y.; Saghir, M.Z.; Lyubimova, T.; Sedelnikov, G.; Roux, B.** (2007): Influence of vibrations on thermodiffusion in binary mixture: a benchmark of numerical solutions, *Physics of Fluids*, vol. 19, p. 017111.

**Yan, Y.; Shevtsova, V.; Saghir, M.Z.** (2006): Numerical Study of Low Frequency G-jitter Effect on Thermal Diffusion, *FDMP: Fluid Dynamics and Material Processing*, vol.1, no 4, pp. 315–328.

**Yan, Y.; Pan, S.; Jules, K.; Saghir, M.Z.** (2007): Vibrational effect on thermal diffusion under different microgravity environments, *Microgravity Science and Technology*, vol. 19, no. 2, pp. 12–25.

**Yan, Y.; Jules, K.; Saghir, M.Z.** (2007): A comparative study of G-jitter effect on thermal diffusion aboard the international space station , *FDMP: Fluid Dynamics and Materials Processing*, vol. 3, no. 3, pp. 231–245.

